ISSN 1392–1320 MATERIALS SCIENCE (MEDŽIAGOTYRA). Vol. 15, No. 3. 2009

Magnetron-Sputter Deposition of W Coatings for Fusion Applications

Liudas PRANEVIČIUS*

Department of Physics, Vytautas Magnus University, 8 Vileikos St., LT-44404 Kaunas, Lithuania

Received 12 December 2008; accepted 19 March 2009

Tungsten (W) is among candidates for the first wall material at critical locations in future fusion reactors. Vicker microhardness, pin-on-disc sliding, wear tests were performed to evaluate the mechanical and tribological properties of the W coatings fabricated by magnetron sputter deposition technique in dependence on the deposition parameters. X-ray diffraction was used for phase and peak shape analysis. The coating morphology was analyzed by scanning electron microscopy. The W coatings with dense microstructure have been developed for applications as wear (or erosion) resistant components.

Keywords: tungsten, coatings, magnetron sputtering, mechanical properties.

1. INTRODUCTION

Low sputtering yields of high atomic number, Z, materials, such as tungsten (W), make them candidates for the first wall material at critical locations in future fusion reactors. W coatings have been developed for applications as wear or erosion resistant components at high temperature [1, 2]. The first wall materials are under special working conditions: temperature – in the range 800 K – 3500 K, a mean power density to the wall of 8 MW/m^2, erosion induced by hydrogen and impurity ions [3]. The erosion of the wall materials leads to: (i) the sputtered particles affect the behavior of plasma, and (ii) the plasma-wall interaction effects modify properties of the wall material.

The divertor is designed to be mostly tungsten. However, carbon layers will be present in certain parts. Thus tungsten is contaminated by carbon where eroded C has drifted to W parts. In this way, the problem can be divided in subproblems: (i) the fabrication of erosion resistive W coatings, (ii) the study of carbon redeposition and its effects on the properties of W coatings, and (iii) the investigation of W erosion kinetics due to hydrogen bombardment, the retention, diffusion and re-emission kinetics of hydrogen isotopes in tungsten contaminated by carbon.

This work is devoted to the optimization of W coating fabrication technology and aims to produce W coatings with improved mechanical erosion properties.

2. EXPERIMENTAL TECHNIQUES

Magnetron sources are widely used for numerous applications where high deposition rate is necessary [4]. Thickness homogeneity, adhesion and microstructure of deposited films are issues of a great importance. In this work, a typical laboratory type planar magnetron sputter deposition system was used. The vacuum chamber was evacuated to a background pressure of 10^{-6} Pa to 10^{-5} Pa by a pumping unit including a cryogenic pump at pumping speed about 150 $\ell \cdot s^{-1}$ for Ar that was controlled by a throttle valve.

In the case of magnetron sputtering source, the magnetron field parallel to the cathode (target) surface is added to trap electrons close to it and consequently to enhance gas ionization by an increase of electron path length in the cathode region. A magnetron source operated with a magnetic field strength of 0.02 T to 0.04 T. The cathode used as a target was made of 99.95 % W (supplier: Kurt J. Lesker). The target diameter – 7.5 cm, the thickness – 6 mm. The target was water cooled.

The mean energy of electrons responsible for working gas (Ar) ionization was about 100 eV, the value close to optimal from the point of view of ionization probability. The discharge current density for this type of discharge was variable in the range from 1 mA·cm^{-2} to 100 mA·cm^{-2} and more. The magnetron discharge current was strongly dependent on cathode-anode voltage, U, and followed relationship $I \sim U^9$. The power dissipated at the cathode was limited by effectiveness of water cooling. The low-pressure limit of operation for W magnetron source was in the range 10^{-1} Pa – 10^{-2} Pa. Magnetron sputter deposition technique includes many variable technological parameters, such as, substrate temperature, deposition rate, working gas pressure, magnetron dissipated power, magnetron discharge current and voltage, and constructive, such as, magnetic field configuration (balanced-unbalanced magnetron), distance target-substrate, cooling system, system for gas inlet, etc. The sample temperature with the accuracy ±5 °C was controlled using the thermocouple attached to the substrate. Without external heating the steady state sample holder temperature was 100 °C – 140 °C during the film deposition, which was reached after two minutes of deposition. Thickness homogeneity, adhesion and structure of deposited films are in complex dependence on the parameters mentioned above.

The fluxes of electrons, ions and neutral particles reaching substrate during film growth strongly influence its morphology, crystal orientation, grain size and internal stress. Usually, for the magnetron sputter deposition the substrate is well outside the dense plasma zone. Thus, it is

* Corresponding author. Tel.: +370-37-327909; fax: +370-37-203858.
E-mail address: *liudas@hydrogen.lt* (L. Pranevičius)

rather difficult to extract ions from it and to use their sufficiently dense fluxes in order to modify film growth conditions on the surface.

In the present work, the distance substrate-target was 3 cm – 4 cm and the substrate was immersed in the magnetron plasma. It allowed to obtain high ion current densities (up to 10 mA·cm^{-2}) from plasma by applying negative bias voltage which was verified in the range from 0 up to the minus 250 V. Plasma parameters, such as, ion flux and electron density were roughly evaluated by a Langmuir probe located at 3 cm above the target. For experimentally controllable parameters, such as: the source power – 200 W, the Ar gas flow rate – 1.1 cm^{-3}·min^{-1} and the substrate temperature – 140 °C, the measured plasma characteristics were the following: the electron concentration – $9 \cdot 10^9$ cm^{-3}, the electron temperature – 2.7 eV, the sheath bias – 10 V and the ion flux – $2.2 \cdot 10^{15}$ cm^{-2}·s^{-1}.

Sample holder was made of stainless steel. Substrates for W films were made of stainless steel and graphite and attached to the sample holder. After deposition of W films their properties were investigated using XRD structural analysis, scanning electron microscopy (JOEL JSM-6300) (SEM) and atomic force microscopy (AFM) surface topography analysis, glow discharge optical emission spectroscopy (GDOES) for compositional and profiling analysis, film resistivity, Vicker hardness and mechanical erosion properties. Film adhesion was evaluated by peel off adhesion test using Scotch tape.

3. EXPERIMENTAL RESULTS

3.1. Adhesion properties of W films on carbon and stainless steel

3.1.1. Fabrication of W films

W films demonstrated a different behavior on stainless steel and on C (graphite) substrates. The substrates were made of high temperature stainless steel Alloy 600 and of the synthetic graphite for nuclear application GR-280. The composition of the stainless steel was as following: 72 at.% Ni, 16 at.% Cr, 8 at.% Fe. The samples had rectangular shape (12 × 20) mm^2 and thickness – 0.5 mm.

Before deposition, the stainless steel and graphite samples received polishing and cleaning surface treatment in trichloroethylene and alcohol using an ultrasonic bath cleaner. The surface roughness of the stainless steel substrates after a final preparation did not exceed 0.02 μm. The SEM surface view of the graphite and stainless steel substrates are shown in Fig. 1. It is seen that graphite includes many pores (Fig. 1, a). The polishing defects are seen for stainless steel surface view shown in Fig. 1, b. The typical W film deposition parameters are presented in Table 1.

Table 1. Deposition conditions for W coatings

Target-substrate distance	(3 – 7) cm
Sputter gas	Ar
Magnetron discharge current	(0.1 – 100) mA·cm^{-2}
Magnetron discharge voltage	(200 – 500) V
Ultimate pressure	< $1 \cdot 10^{-5}$ Pa
Sputter gas pressure	(0.4 – 5) Pa
Deposition rate	(1 – 20) nm·s^{-1}
Deposition time	(15 – 90) min
Substrate bias	0 to – 250 V
Substrate temperature	(110 – 300) °C

The shutter was used to prevent W deposition during target ion bombardment precleaning procedure (t = 10 min, j_i = 1.0 mA·cm^{-2} and V_{bias} = –200 V). The film thickness was monitored by weight method using microbalance with a weight uncertainty of 2 μg.

3.1.2. W films on stainless steel substrate

The W films on stainless steel substrates with thickness less than 2 μm demonstrated good adhesion properties in the wide range of deposition parameters: 0.4 Pa – 2 Pa pressure, negative bias in the range –(50 – 150) V, substrate temperature – 50 °C – 200 °C and distance target substrate 5 cm – 7 cm. However, the adhesion failure for the W films with thickness 5 μm and more was registered in many cases using classical magnetron sputter deposition technology when distance target-substrate was equal to 5 cm – 7 cm and more. Fig. 2 illustrates typical surface view of the W film after the adhesion failure: film thickness – 4 μm, deposition rate – 4 nm·s^{-1}, substrate temperature – 110 °C, substrate-target distance – 7 cm.

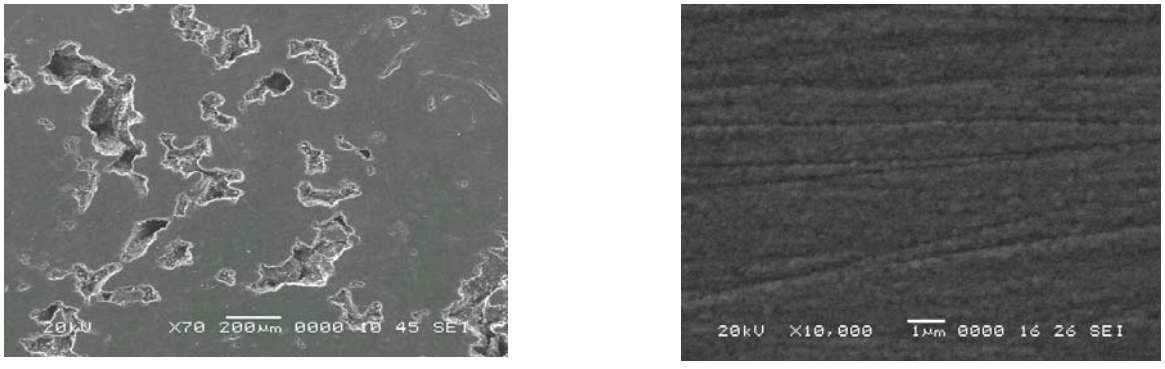

a b

Fig. 1. The SEM surface view of the graphite substrate (a) and stainless steel substrate (b) before W film deposition

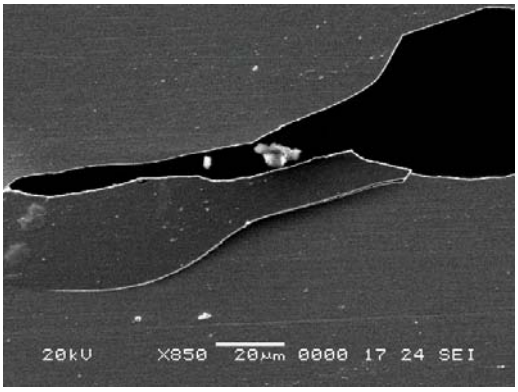

Fig. 2. SEM surface view of 4 µm-thick W film deposited at 2 Pa, $V_{bias} = -100$ V and the distance target-substrate – 7 cm

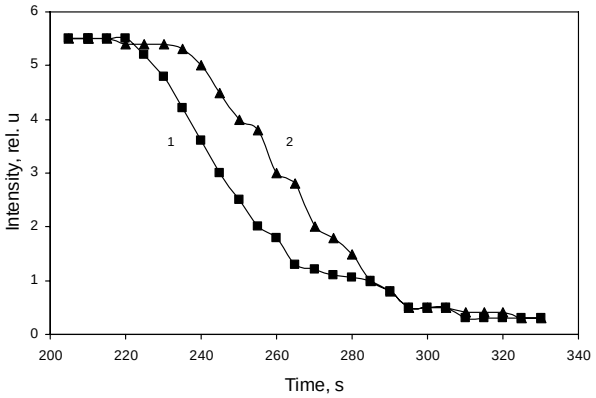

Fig. 3. The W distribution profiles for 5 µm-thick W film grown on the steel substrate located at 4 cm (curve 1) and 7 cm (curve 2) above the target

The significant improvement of adhesion properties has been achieved with the increase of ion irradiation intensity of growing film during deposition. It was achieved by the decrease of distance target-substrate when substrate practically was immersed in magnetron plasma and surrounded by it. Significant improvement of adhesion properties was registered for the distance target-substrate equal to 3 cm – 4 cm. The 7 µm-thick W films well adhered to stainless steel substrate have been fabricated. The rough evaluations gave that during this deposition regime the ratio of incident ions to neutrals was about 0.2. The negative bias voltage during deposition was –100 V. It is known [5, 6] that under these conditions intermixing of substrate material and deposited atoms take place. It results in the formation of an altered mixed layer at the film-substrate interface.

Fig. 3 illustrates W distribution profiles across interface film-substrate region obtained using GDOES technique: curve 1 – for the W film grown on the substrate located 4 cm above the target, and curve 2 – for W film deposited by classical magnetron sputter technology (deposition rate – 4 nm·s^{-1}, substrate temperature – 110 °C, substrate-target distance – 7 cm). The broadening of the distribution profile may be interpreted as the intermixing of film and substrate atoms. It supports the suggestion that the improvement of adhesion properties is achieved due to formation of mixed interface layer.

3.1.3. W film on C (graphite) substrate

The bond between film and substrate may fail by several reasons. It is useful to distinguish two types of stress: tensile stress, effective perpendicularly to the interface, and shear stress, appearing along the plane of contact. Film material may inhibit rigidity higher than that of the substrate. Under such conditions, fracture will occur within the substrate. Cohesive failure will be the consequence if the adhesion at the interface surpasses the cohesion of the substrate material.

It is the case of W film on the graphite substrate. The W films of 1 µm – 2 µm thickness were reliably grown on the graphite substrate. The W films of 5 µm – 7 µm thickness on the graphite demonstrated lack of adhesion (7 of 10 films were pilled off). However, the nature of the adhesion failure was different from that one observed for W films on the stainless steel substrate. It was registered that for W films grown on C substrate under low intensity ion irradiation (distance target-substrate 7 cm) the adhesion failure is the result of the weak bonding at the interface (Fig. 4, a), and for W films grown on C substrate under high intensity ion irradiation (distance target-substrate 4 cm) the adhesion failure is the result of the cohesive failure in the graphite (Fig. 4, b).

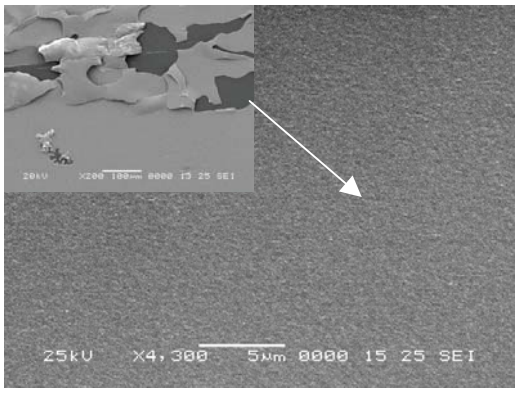

a

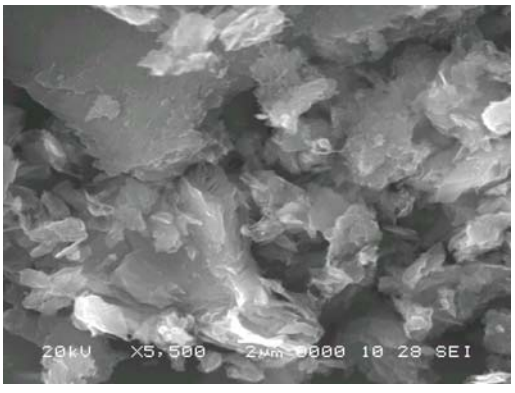

b

Fig. 4. SEM surface views of W film on graphite after adhesion failure: a – at the interface (an insert), and b – after cohesive lift off of W film

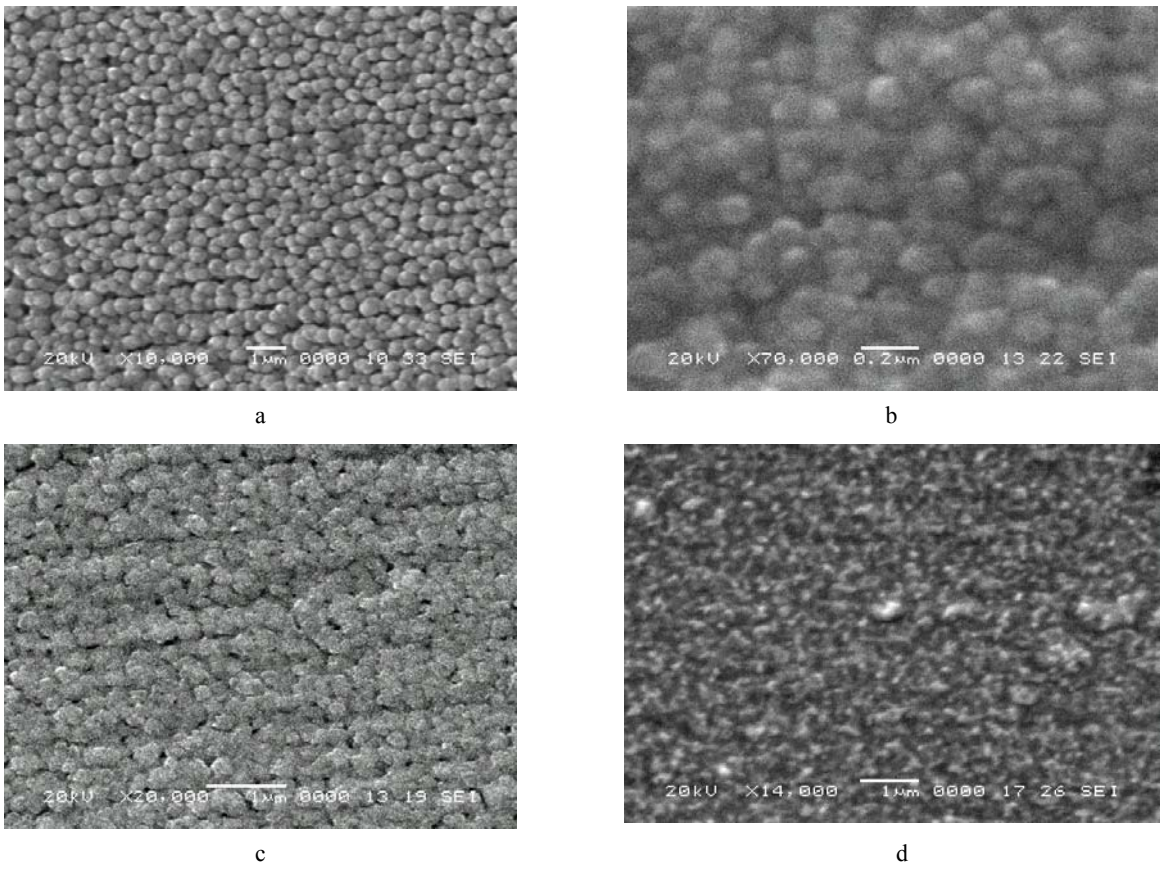

a b

c d

Fig. 5. SEM surface views of 2 μm thick W coatings produced under different bias voltages: a and c – $V_{bias} = 0$ V, and b and d – $V_{bias} = -100$ V for stainless steel substrate (a and b) and graphite substrate (c and d)

The observation of cohesion failure indicates to the attainment of the optimum adhesion. Further improvements of the system W-graphite should be sought in the direction of increasing the inherent strength of the substrate material.

3.2. Coating density

All W coatings were analyzed by SEM and showed a columnar microstructure as it was expected for metal coatings deposited under low adatom mobility conditions. Increasing particle bombardment of the growing film due to negative substrate potential changes significantly the coating microstructure.

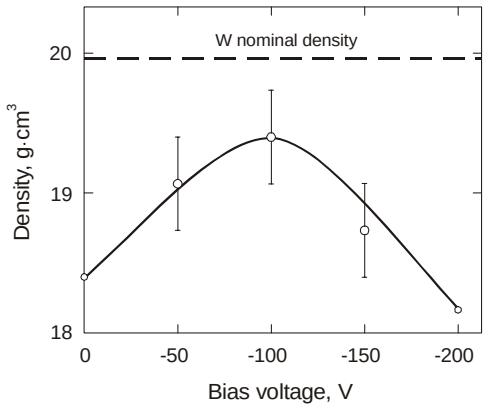

Fig. 6. The dependence of W-coating density as a function of the bias voltage

In Fig. 5 SEM shows surface views of W coatings produced under different bias voltages. The micrographs suggest an increasing densification of the W coatings. These results have been confirmed by weight gain measurements.

Fig. 6 demonstrates the change of W-coating density as a function of the bias voltage. The dotted line presents the W nominal density. The density was strongly dependent on the ion energy. A maximum of 19.4 g·cm^{-3} occurred at approximately 100 eV. The density increase at low energy was due to bombardment enhancement. Beyond 100 eV, the decrease may be attributed to a competing damage effect induced by the cascade collisions and vacancy creations which becomes more and more important and finally dominates when the energy is increased.

3.3. Preferred crystallographic orientation

In the present work the microstructure of films was analyzed by X-ray diffraction with the 2Θ angle in the range 20º – 90º using CuK_α radiation in steps of 0.05º. Peak positions and full width of peak at half minimum of intensity were obtained by fitting the measured peaks with two Gaussian curves in order to find the true peak position and width corresponding to monochromatic $K_{\alpha 1}$ radiation. A qualitative texture analysis of the W-coatings was made by comparison of the measured X-ray peak intensities with those obtained for bulk material, for example, of the sputtering target. The identification of phases was performed using Crystallographic Search-Match program.

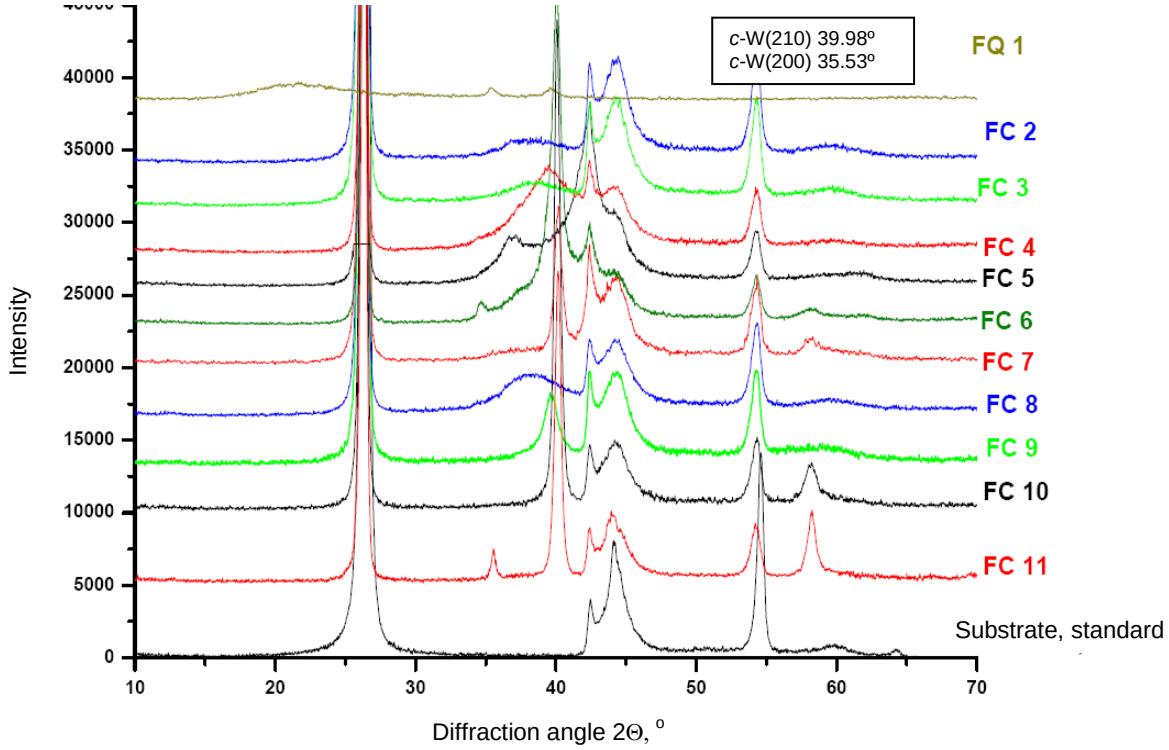

Fig. 7. The XRD patterns (FC2 – FC11) of the W films on the graphite and on the quartz (FQ1) substrates for different film deposition parameters: FC2 – V_{bias} = –250 V, FC3 – V_{bias} = –230 V, FC4 – V_{bias} = –180 V, FC5 – V_{bias} = –150 V, FC6 – V_{bias} = –120 V, FC7 – V_{bias} = –100 V, FC8 – V_{bias} = –50 V for working gas pressure 0.5 Pa, and FC9 – V_{bias} = –120 V, FC10 – V_{bias} = –100 V and FC11 – V_{bias} = –80 V for the working gas pressure 0.5 Pa

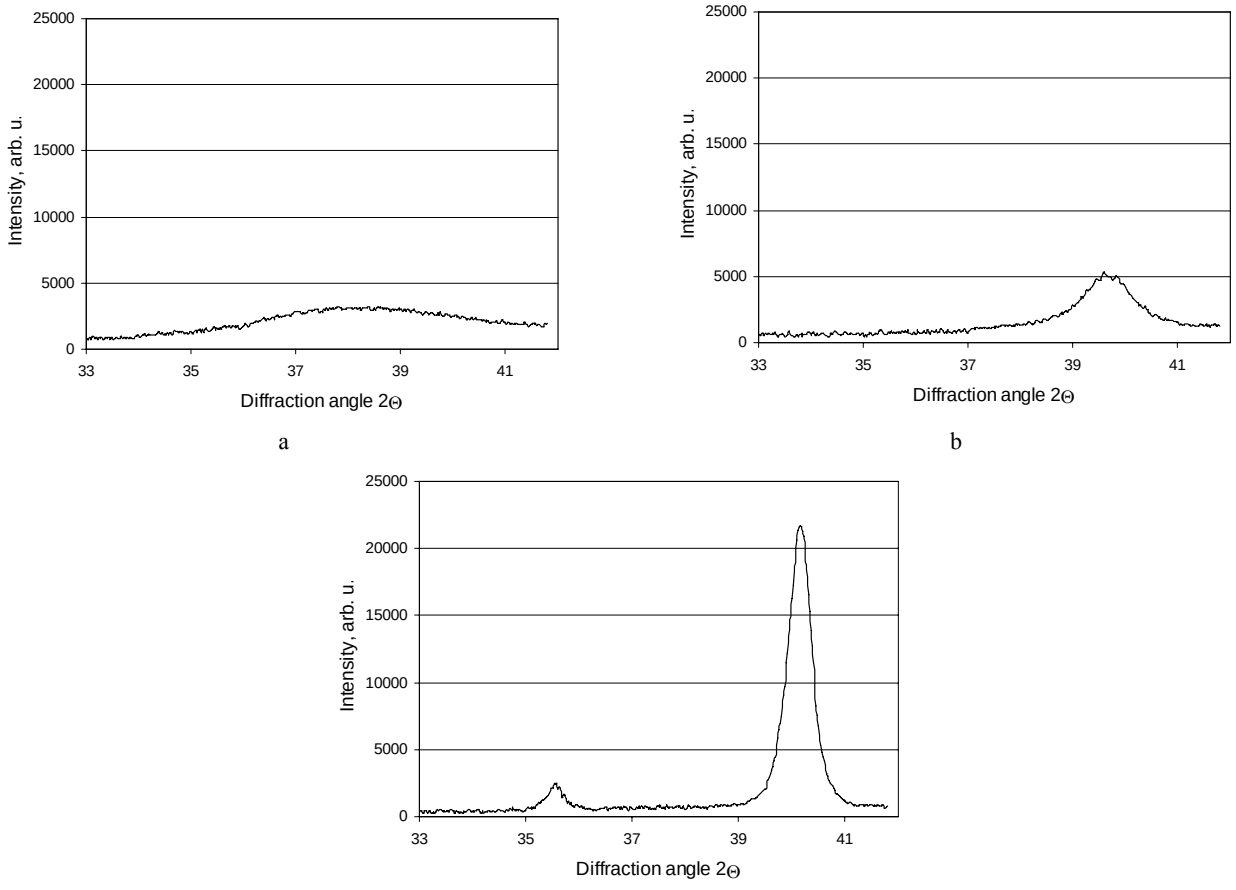

Fig. 8. The XRD patterns of grown W films for different applied substrate negative bias: a – 200 V, b – 50 V and c – 100 V

The XRD patterns of as-deposited W films exhibited diffraction peaks at diffraction angles matching with those of the α and β-W phases. The average crystallite dimension of films, D, was calculated using the formula $D = 0.9\,\lambda\,(\beta\cos\Theta)^{-1}$ neglecting the microstrain, where λ is the X-ray wavelength, Θ is the Bragg diffraction angle and β is the full-width of the peak after correcting for the instrument broadening. The films demonstrated nanocrystalline structure with the mean size of crystallites in the range 40 nm – 70 nm.

Fig. 7 includes the XRD patterns (FC2 – FC11) of the W films on the graphite and on the quartz (FQ1) for the analysis of optical properties for the different values of bias voltages and working gas pressures.

The XRD pattern of the graphite substrate is included (curve is denoted as *Substrate*). Polycrystalline randomly oriented W crystallites (powder standard) present diffraction peaks (with decreasing intensity) for the *c*-(210) at $2\Theta = 39.98°$, *c*-(211) at $2\Theta = 44.02°$ and *c*-(200) at $2\Theta = 35.53°$ crystallographic planes. The position of the experimentally measured diffraction peaks at $2\Theta = 39.98°$ and $2\Theta = 35.53°$ are slightly towards the low value of diffraction angles. The dilatation of the crystal lattice of about 1.1 % may result from internal stresses in the sputter deposited films. W coatings produced at pressure $5\cdot10^{-1}$ Pa under intensive Ar ion irradiation are strongly textured with (210) crystallographic plane.

Fig. 8 XRD shows predominant diffraction peak at $2\Theta = 39.98°$ for W coatings produced for different applied substrate bias. Coatings grown under –200 V bias are almost X-ray amorphous. Apparently, the intensive ion bombardment of the growing film destroyed the growing crystallites, but not the columnar structure. It seems, that all recrystallization processes after film growth are effectively suppressed. At intermediate bias voltage (50 V – 150 V) the enhanced bombardment favors the texturing of the W coating. The textured crystallinity is well expressed and the mean size of crystallites is in the range 20 nm – 50 nm for W films demonstrating good adhesion properties ($V_{bias} = -100$ V, distance target-substrate – 4 cm).

For grown W films, the main Bragg reflection was observed located at $2\Theta \sim 39.9°$, and in some cases small peak at $2\Theta \sim 35.5°$. The peak at $2\Theta \sim 39.9°$ may be attributed to one or both (210) β-W and (110) α-W reflections. The relatively large peak width suggests the presence of a mixture β-W and α-W phases. The α-W phase (*bcc*) is the thermodynamically stable phase, while the β-W phase has been identified as a metastable form of pure tungsten, being of a faulted W_3-W type, while other authors pretended that it is a tungsten oxide of W_3O type. The occurrence of a β-phase has been observed previously in sputtered W films [7].

In some cases small peak at $2\Theta \sim 35.5°$ was registered corresponding to β-W only. It indicates that ion irradiation tend to decrease and suppress the formation of β grains.

3.4. Electrical resistivity

The film resistance of W films was determined by four point probe measurements. The electrical resistivity was deduced from the values of sheet resistance and thickness of films.

The electrical resistivity of film is a parameter sensitive to the microstructure of film presence of impurities in it. For all fabricated films, it has been registered that electrical resistivity of film is lower than the resistivity of bulk material (5.8 μΩ·cm).

Fig. 9 shows the film resistivity dependence on the bias voltage for the working gas pressure equal to 0.4 Pa. Since for all cases the coating thickness exceeded the mean free path of the conduction electrons, the scattering of electrons with surface it is not the dominant mechanism that influence on electrical resistivity. The higher resistivity observed in the coatings is attributed to the scattering of electrons by structural defects (e. g. vacancies, interstitials and grain boundaries) and impurities (e. g. oxygen, nitrogen and argon). With increasing ion energy up to 100 eV – 120 eV the level of impurity content decreases as sputtering begins, the voids in the film decreases and therefore the electrical resistivity decreases. Probably, the oxygen incorporation in the more porous films when they are exposed to atmosphere after the deposition process can also be responsible for the higher electrical resistivity observed.

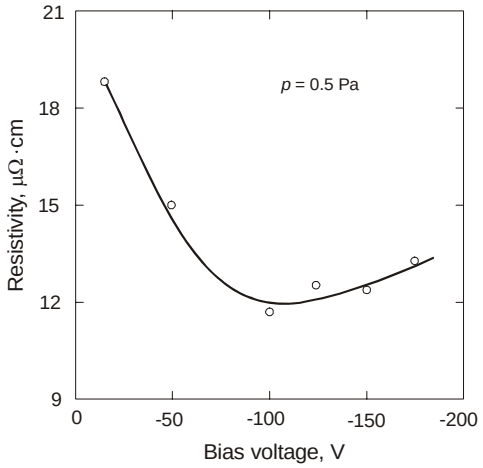

Fig. 9. The film resistivity dependence on the bias voltage

The minimum electrical resistivity value was obtained from W films with no internal stress.

3.5. Mechanical properties

The mechanical (Vicker hardness and erosion resistance) properties of deposited W films have been investigated. Microhardness properties have measured using Vicker indentation technique, and erosion resistance properties – using pin-on-disc technique. Surface topography has been studied by two- and three-dimensional profilometer (Talysurf 10) and SEM. The studies of mechanical properties have been performed in collaboration with the Laboratory of Metallurgy Physics of the Poitiers University, France under supervisor of prof. Claude Templier.

3.5.1. Vicker hardness

Method is based on the measurements of penetration depth, h_{max}, of identor under applied force. It was used

diamond identor of the pyramid shape with angle 136º. The microhardness in Pa was estimated as $HV = 1.85\,P/d^2$, where P is the applied force (in N), and d is the diagonal of the square formed by identor. In the present work the 5 g and 50 g loads were used.

The experimental results are summarized in Table 2. It includes information about the variable parameter V_{bias} for other parameters such as: working gas pressure – 0.4 Pa, film thickness – 5 μm on stainless steel substrate, substrate temperature during deposition – 110 ºC, and the distance target-substrate – 4 cm.

Table 2. Vicker hardness versus negative bias voltage

V_{bias}, V	Load 50 g		Load 5g	
	h_{max}, μm	HV, GPa	h_{max}, μm	HV, GPa
0	1.36	1.4	0.42	1.4
–50	1.26	1.6	0.35	2.1
–100	1.32	2.6	0.24	5.4
–150	1.26	1.6	0.25	5.1
–200	1.29	2.2	0.30	3.2

Vicker hardness measurements showed the increase in hardness for W films grown at $V_{bias} \approx -100$ V. The deeper understanding of the hardness improvement mechanism may be related to the coating restructuring processes.

3.5.2. Erosion resistance

The mechanical erosion properties of W films have been studied using the pin-on-disc technique. The acting applied force was verified in the range from 2.4 N to 8 N, the rotation speed – 10 rotations per min, the linear speed – 8 mm·s^{-1}, and the total number of rotations – 4000. The 5 μm-thick W films on stainless steel substrates were fabricated at working gas pressure – 0.4 Pa, temperature – 110 ºC, and the distance target-substrate – 4 cm for different bias voltage.

The SEM surface topography of the eroded W film is shown in Fig. 10.

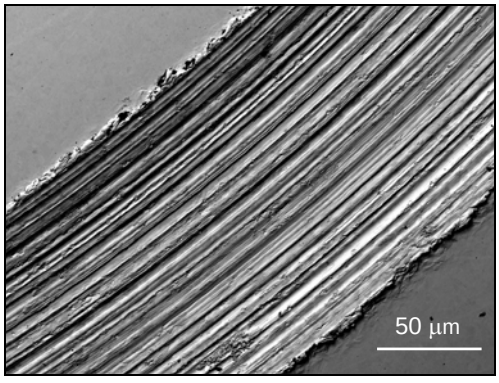

Fig. 10. The SEM surface view of a track formed by a pin erosion

Fig. 11 illustrates erosion profiles after 4000 rotations under acting force 8 N for W films grown under V_{bias} = = –50 V (Fig. 11, a) and –100 V (Fig. 11, b).

The maximum erosion depth for W film grown under $V_{bias} = -50$ V may be estimated as approximately equal to 1 μm. The maximum erosion depth for W film grown under $V_{bias} = -100$ V decreased up to 0.75 μm. It was registered that the wear resistance properties correlated with the film density. W films grown under intensive high-flux, low-energy ion irradiation demonstrated improved mechanical properties.

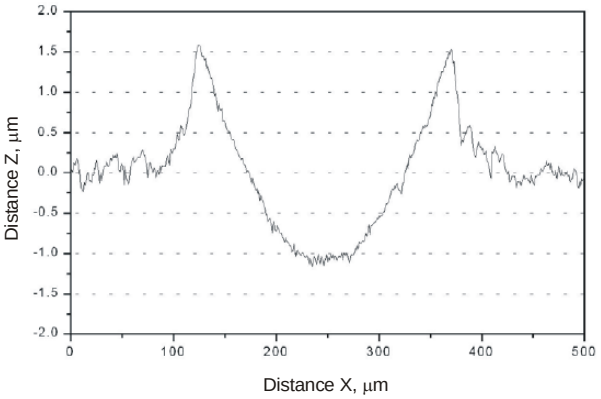

a

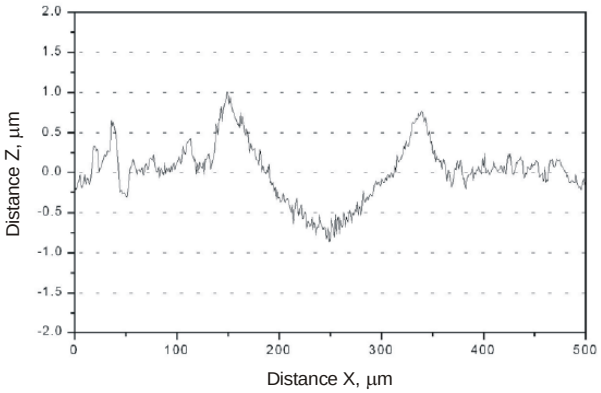

b

Fig. 11. The erosion profiles for W film after 4000 rotations under acting force 8 N grown under different V_{bias}: a – 50 V, and b – 100 V

4. CONCLUSIONS

This work has demonstrated the possibility of fabrication (3 – 7) μm-thick tungsten films well adhered to the stainless steel substrate and having improved wear resistance properties. The films were fabricated employing DC magnetron sputtering technique under high-flux and low-energy Ar ion irradiation. The optimum parameters: Ar working gas pressure – 0.4 Pa – 0.6 Pa, bias voltage – (80 – 100) V, deposition rate – (6 – 8) nm·s^{-1}, substrate temperature – 110 ºC, distance target-substrate – 4 cm, magnetron discharge current – 200 mA, magnetron discharge voltage – 300 V, ratio of fluxes of incident ions to neutrals – 0.2 – 0.4.

The W films with the thickness exceeding 2 μm on graphite substrates demonstrated cohesive adhesion failure.

An attempt to explain the observed improvements of film mechanical properties has been made. The assumption is made that under high-flux, low-energy ion irradiation when ratio of fluxes of incident ions to neutrals, F_i/F_n, is approximately 0.2 – 0.4 the dominant processes inducing restructuring of growing film are related to enhancement of relocation of W film surface atoms and their continuous

mixing with arriving W atoms. When $F_i/F_n < 0.2$ the role of ion irradiation induced mixing diminishes, and the ion irradiation effects are mainly related to primary ion interaction effects.

Acknowledgement

This work was performed in the framework of the specific programme (Euroatom) for research and training on nuclear energy (acronym FU06-CT-2005-00074) and was supported by the Lithuanian National Foundation. The authors are grateful to prof. C. Templier of the Metallurgy Physics Laboratory, Poitiers University, France, for providing facilities to perform measurements of mechanical properties.

REFERENCES

1. **Gachon, Y., Ienny, P., Forner, A., Farges, G., Sainte Catherine, M. C., Vannes, A. B.** Erosion by Solid Particles of W/W–N Multilayer Coatings Obtained by PVD Process *Surface and Coatings Technology* 113 1999: pp. 140 – 148.
2. **Esteve, J., Zambrano, G., Rincon, C., Martinez, E., Galindo, H., Prieto, P.** Mechanical and Tribological Properties of Tungsten Carbide Sputtered Coatings *Thin Solid Films* 373 2000: pp. 282 – 286.
3. Fusion Year Books. *Annual reports 2003 and 2004* (Eds. Seppo Kattunen, Karin Rantamaki), VTT, Finland.
4. **Pranevičius, L. L.** Vapor Deposition Coating Technologies. In: Coatings Technology Handbook. 3rd edition (Ed. Tracton, A. A.), Boca Taylor and Francis Group, Raton, FL., 2005: pp. 31.1 – 31.30.
5. **Galdikas, A., Pranevičius, L.** Interactions of Ions with Condensed Matter. *Horizons in World Physics* Vol. 229 Nova Science Publishers, Inc., New York, 2000: 176 p.
6. **Nastasi, M., Mayer, J. W., Hirvonen, J. K.** Ion-Solid Interactions, Fundamentals, and Applications. Cambridge Solid State Science Series, Cambridge University Press, 1996: 540 p.
7. **Villain, P., Goudeau, P., Ligot, J., Benayoun, S., Badawi, K. F., Hantzpergue, J. J.** X-ray Diffraction Study of Residual Stress and Microstructure in Tungsten Thin Films Sputter Deposited on Polyimide *Journal of Vacuum Science Technology* A 21 (4) 2003: pp. 967 – 972.

DOI: 10.5755/j02.ms.26151